# CEOCOR

**Madrid (Spain)**

**May 25th – May 28th, 2021**

**Paper 2021-21**

# Role of bicarbonate ions and iron bacteria in forming tubercle relevant to graphitic corrosion of ductile iron

*by F.Kajiyama (Tokyo Gas Pipeline Co, Tokyo, Japan)*

# Role of bicarbonate ions and iron bacteria in forming tubercle relevant to graphitic corrosion of ductile iron

Fumio Kajiyama, Dr.
Tokyo Gas Pipeline Co., Ltd., 1-5-20, Kaigan, Minato-ku, Tokyo 105-8527, Japan

## Abstract

We experienced natural gas low pressure ductile iron pipe corrosion as high as 0,384 mm/y in aerobic soil with highly alkalinity that had been considered to be mildly corrosive as per AWWA C105-10. To clarify this phenomenon, burial test of a ductile iron coupon was carried out in the same soil. Analyses of corrosion site of the coupon were made using electron probe microanalyzer and X-ray diffraction. Iron bacteria were identified. Other bacteria such as sulphate-reducing bacteria were enumerated. Electrochemical techniques using corrosion potential, electrochemical impedance spectroscopy (EIS), and polarization curves were also applied to this study. In this paper, particular emphasis is placed on the role of bicarbonate ions and iron bacteria in forming tubercle relevant to graphitic corrosion of ductile iron.

## 1 Introduction

The author reported natural gas low pressure ductile iron pipe corrosion as high as 0,384 mm/y in aerobic soil at pH 8,25 was observed [1]. Pits developed forming graphitic corrosion within the growing tubercles. The soil contained bicarbonate ions of the concentration of 456 mass ppm and bacteria such as iron bacteria, iron-oxidizing bacteria. In fully deaerated conditions containing active sulphate-reducing bacteria,

tubercles on ductile iron pipes are not formed [1]. So, a question arises whether tubercles are formed as long as soils are aerobic. This paper struggles with this question using the microscopic inspection of corrosion pit together with tubercle, and chemical, electrochemical, and microbiological techniques in the laboratory. Possible mechanism on the formation of stabilized tubercle and pit was also studied by taking chemical and biochemical reactions into consideration.

## 2 10-point soil evaluation system

Bare ductile iron is susceptible to severe corrosion when installed in aggressive environments. In the case of ductile iron in soil, the extent of corrosion is influenced by soil corrosivity. Based upon this, the 10-point soil evaluation procedure was instituted by the Cast Iron Pipe Research Association (CIPRA) in 1964 to predict conditions corrosive to underground piping [2], [3]. CIPRA became the Ductile Iron Pipe Research Association (DIPRA) in 1979. The 10-point soil evaluation system is intended as a guide in determining soil corrosivity to corrode ductile iron pipe.
The evaluation procedure is based upon five soil factors. For a given soil sample, each factor is evaluated and assigned points. The American Water Works Association (AWWA) developed points according to its contribution to corrosivity, applicable to ductile iron as shown in Table 1 [4]. If total points are ten or greater, the soil is considered corrosive to ductile iron and protection such as polyethylene encasement and/or cathodic protection is needed.

The soil used for this laboratory study was collected from the field at the same location, and then soil corrosivity was evaluated as per AWWA C105-10.

Table 1 AWWA C 105−10 10-point soil evaluation system [4].

| Soil characteristics | Values | Point |
|---|---|---|
| Resistivity (Ωcm) | <1500 | 10 |
| | 1500−1800 | 8 |
| | 1800−2100 | 5 |
| | 2100−2500 | 2 |
| | 2500−3000 | 1 |
| | >3000 | 0 |
| pH | 0−2 | 5 |
| | 2−4 | 3 |
| | 4−6.5 | 0 |

| | | |
|---|---|---|
| | 6.5−7.5 | 0 * |
| | 7.5−8.5 | 0 |
| | >8.5 | 3 |
| Redox potential (mV) | <0 | 5 |
| | 0−50 | 4 |
| | 50−100 | 3,5 |
| | >100 | 0 |
| Sulfides | Positive | 3,5 |
| | Trace | 2 |
| | Negative | 0 |
| Moisture | Poor drainage, continuously wet | 2 |
| | Fair drainage, generally moist | 1 |
| | Good drainage, dry | 0 |

*If sulphides are present and low (<100 mV) or negative redox potential results are obtained, add three points for this range.

In contrast to the 10-point soil evaluation system, DIN 50 929 was published in 1985 intended to serve as a basis for estimating the probability of corrosion of metallic pipelines, vessels and structural components whose external surfaces are contact with soil or surface water [5].

## 3 Laboratory study procedures

### 3.1 EPMA of a cross section of localized corrosion

A cross section of localized corrosion on a 150 mm diameter, 8,5 mm wall thickness natural gas low pressure ductile iron pipe exposed for a period of 17 years to the soil used for 10-point soil evaluation test was examined using EPMA (Electron Probe Microanalyzer) .

### 3.2 X-ray diffraction analysis of the tubercle and residue in the corrosion pit

X-ray diffraction analysis of the tubercle and residue in the corrosion pit was made.

### 3.3 XPS analysis of a substance containing silica in the corrosion pit

XPS (X-ray Photoelectron Spectroscopy) analysis was made on a substance containing silica in the corrosion pit.

### 3.4 Burial testing of ductile iron coupon for a period of 30 and 90 days

To confirm the reproduction of the corrosion result of field, a corrosion testing was made by burying a ductile iron coupon plate having a surface area of 6 $cm^2$ (20 mm width, 30 mm height, and 8 mm thickness) in the soil shown in table 2 described in 4.1. Burial testing included :

- observation on a  a cross section of ductile iron coupon exposed for a period of 30 days to the soil using EPMA ;
- electrochemical measurements on ductile iron coupon exposed for a period of 90 days to the soil and bacterial enumeration.

### 3.5 Electrochemical techniques and enumeration of bacteria

Electrochemical techniques were applied to this study. These techniques included 1) corrosion potential, 2) electrochemical impedance spectroscopy (EIS), and 3) polarization curves. Electrochemical techniques employed for a period of 90 days used a three-electrode configuration comprised of ductile iron coupon plate electrodes, one of which was a working electrode having the same surface area used in the 30-day testing.

Before and after the 90-day testing, iron bacteria were cultivated. Sulphate-reducing bacteria, iron-oxidizing bacteria, and sulfur-oxidizing bacteria were enumerated [6], [7]. Enumeration of iron-oxidizing, sulphur-oxidizing, and sulphate-reducing bacteria was by the standard Most Probable Number Technique and iron bacteria were observed with the aid of electron microscope. It is important to remember that, iron-oxidizing bacteria (IOB, *Thiobacillus ferrooxidans*) oxidize $Fe^{2+}$ to $Fe^{3+}$ and produce $H_2SO_4$ within the optimum acid region of pH 2,0 to 2,5, whereas iron bacteria (IB, *Leptothrix*, *Gallionella*, etc,) oxidize $Fe^{2+}$ to $Fe^{3+}$ to form tubercle near the neutral pH. Iron-oxidizing bacteria and iron bacteria are aerobic.

#### 3.5.1 Corrosion potential

Corrosion potential of a working electrode was measured with respect to copper sulphate electrode (CSE).

#### 3.5.2 EIS

For EIS measurements a frequency response analyzer (FRA) together with a potentiostat were used. The frequencies ranged from 10 kHz to 1 mHz. Upon conclusion of burial testing, the ductile iron coupon was removed from the soil, followed by cleaning and mass loss measurement. The mass loss measurement was converted into general corrosion rate by applying Faraday's Law. Furthermore, maximum corrosion rate was obtained from the measurement on maximum corrosion depth.

### 3.5.3 Polarization curves

The first measurement was that of the corrosion potential $E_{corr}$ when the applied current was zero. Using the potentiostat, the working electrode was then potentiostatically polarized either in anodic and cathodic steps. IR drop was completely eliminated.

## 4 Results and discussion

### 4.1 10-point soil evaluation system

Table 2 shows the results of 10-point soil evaluation for a sample used for this study.

Table 2 Results of 10-point soil evaluation for a sample used for this study.

| Factor | Value | Pont |
|---|---|---|
| Resistivity (Ωcm) | 5230 | 0 |
| pH | 8,25 | 0 |
| Redox potential (mV) | 399 | 0 |
| Sulfides | Positive (193 mass ppm) | 3,5 |
| Moisture | Poor drainage, continuously wet (24,5 %) | 2 |

As a result of this investigation, a total of five factors was 5,5. Therefore, the soil was considered mildly corrosive to ductile iron, and protective measures need not to be taken. However, as will be mentioned later, maximum corrosion rate was 0,284 mm/y that was considered to corrosive to ductile iron. It is not intended here to discuss the correlation between the rate of ductile iron pipe corrosion and 10-point value of the soil.

The concentration of $HCO_3^-$ ions was 326 mass ppm. The $CO_2$ concentration from decomposing organic matter in the soil is higher than that in the atmosphere. $CO_2$ in the soil readily dissolves in the high pH soil solution and forms a concentrated mixture of bicarbonate and carbonate in the pH range of 8 to 11.

### 4.2 EPMA of a cross section of localized corrosion on ductile iron pipe

Figure 1 shows EPMA of a cross section of localized corrosion on 150 mm diameter ductile iron pipe exposed for a period of 17 years to the soil shown in Table 2.From maximum depth of corrosion, maximum corrosion rate was determined as 0,284 mm/y. The map of EPMA (Electron Probe Microanalyzer) shows that, the closer the dot with deeper white, the higher concentration of the element. It is noticed that a large hemispherical pit, 18 mm in diameter, is covered with massive tubercle consisting mainly Fe−O compound and Si. Tubercles were observed above the 3 to 9 o'clock position of the ductile iron pipeline.

Particularly noteworthy is that :

- At the localized corrosion area (pit), high concentration of elements of O, Si, S, and C is observed ;
- Within the tubercle, high concentration of elements of O, Si, Fe, and S is observed. From the pit to the outer surface of the tubercle, element S is observed, indicating that the anion including S such as $SO_4^{2-}$ can mitigate in the tubercle and pit, due to permeability of tubercle to ions. The element distribution of O, Si, and Fe increases as closer to the metal surface ;
- The elements of Si and O sustain the shape of the tubercle.

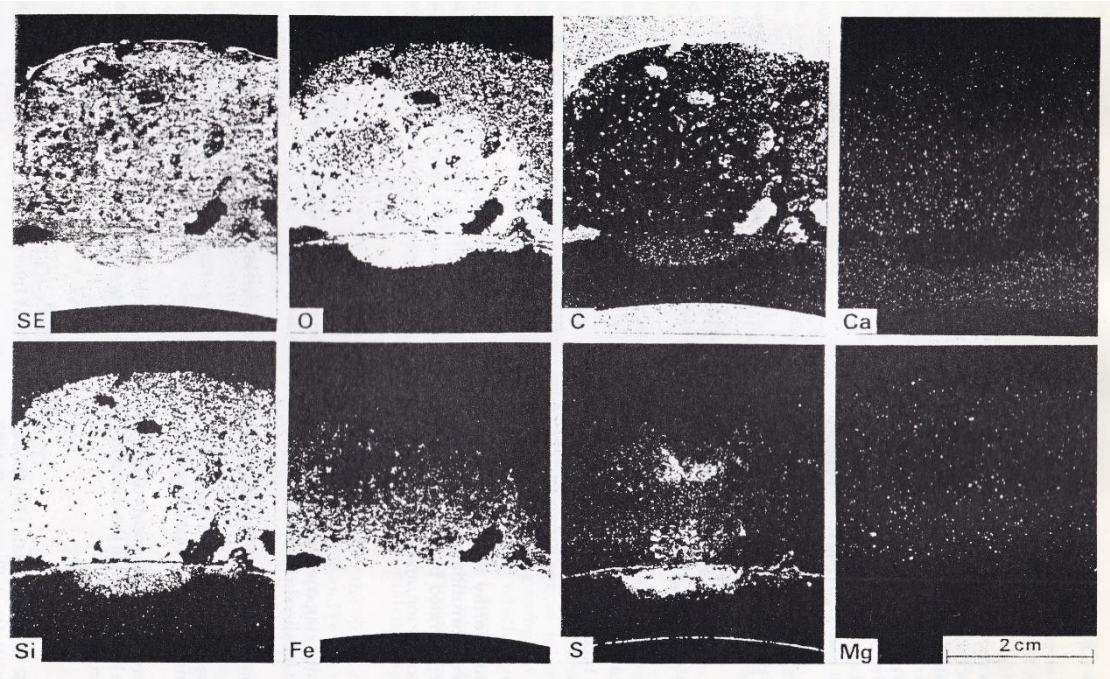


Figure 1 EPMA of a cross section of a localized corrosion on 150 mm diameter ductile iron pipe exposed for a period of 17 years to the soil shown in Table 2 [8].

Figure 2 shows a close-up of Figure 1 at the bottom of the corrosion pit. The results show selective corrosion, resulting in partial removal of iron, leaving spheroidal graphite. Therefore, ductile iron pipe corrosion is a form of graphitic corrosion. It is noteworthy that Si is enriched around the spheroidal graphite.

By taking the observations of Figures 1 and 2, the following can be summarized :

- Graphitic corrosion forms pit comprising of O, Si, S, and C.
- Anions including Si and S (ex. $H_3SiO_4^-$, $SO_4^{2-}$, etc.) can migrate to the metal surface.

The observed element of O may be consist of Fe−O compound, and constituent of anions such as $H_3SiO_4^-$, $SO_4^{2-}$, $HCO_3^-$, and $CO_3^{2-}$.

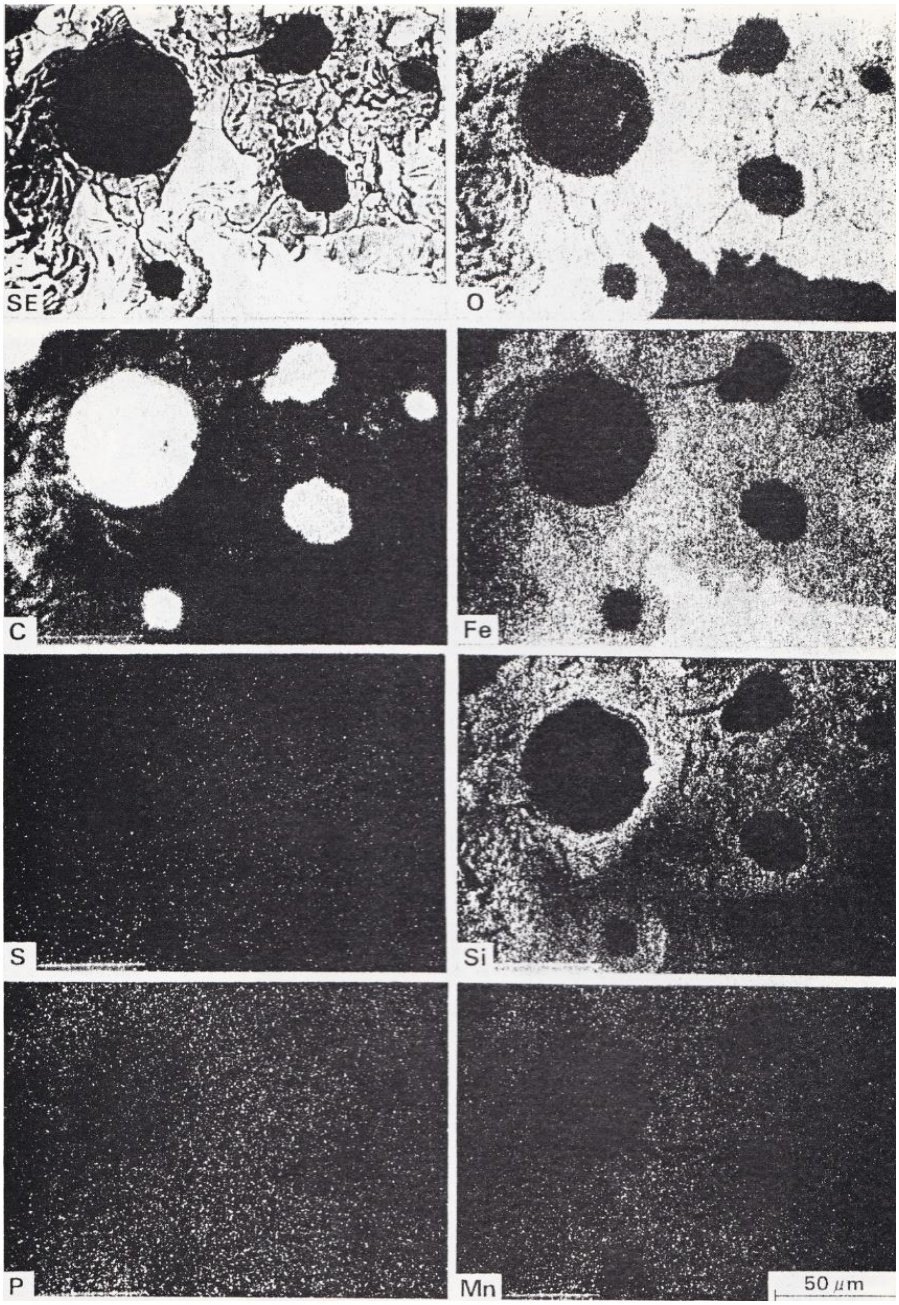


Figure 2 Close-up of Figure 1 at the bottom of the corrosion pit [8].

### 4.3 X-ray diffraction analysis of the tubercle and residue in the corrosion pit

The X-ray diffraction analysis in the tubercle showed it to be ϒ-FeOOH. Analysis of X-ray diffraction of the residue in the corrosion pit given in Figure 3 identified siderite, C, and Si. Siderate which is often observed in microbiologically influenced corrosion.

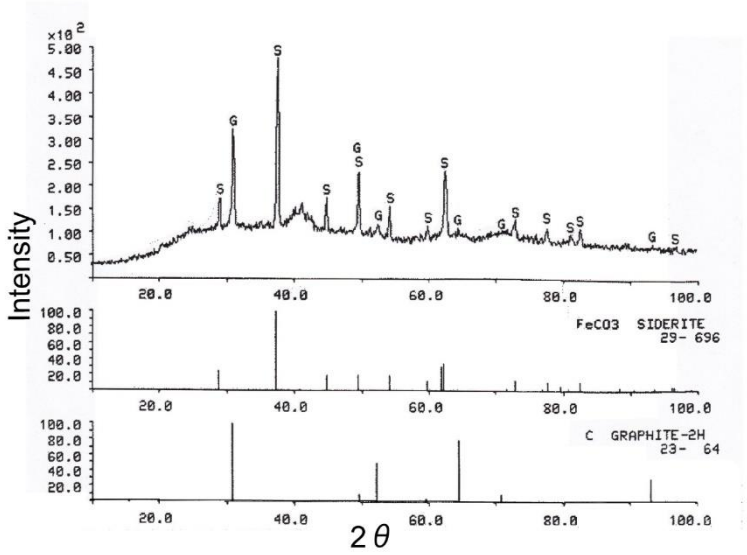


Figure 3 X-ray diffraction analysis of residue in the corrosion pit [9].

### 4.4 XPS analysis of silica in the corrosion pit

As seen in Figure 1, high concentration of Si (silica) is observed both in the pit and tubercle. Furthermore, a compound of silica is not detected by X-ray diffraction analysis as shown in Figure 3. Therefore, silica in the pit can be regarded as a form of amorphous. So XPS analysis of the amorphous silica in the pit was made. As a result, the Si (2p) binding energy of 102,6 eV was obtained, indicating the same as glass. In 2017, Igarashi and Sato presented a paper titled 'The world's first elucidation of orthosilicic acid, basic unit of glass' [10]. These lead to the conclusion that amorphous silica in the corrosion pit is considered to be orthosilicic acid. The same conclusion applies to the substrate which consists of silica, because some ions can migrate between the pit and tubercle through the mouth of the pit.

### 4.5 Reproduction of graphitic corrosion on ductile iron coupon

Figure 4 shows EPMA of a cross section of ductile iron coupon exposed for a period of 30 days to the soil shown in Table 2. The maximum localized corrosion depth of 0,12 mm, that is, maximum corrosion rate of 1,41 mm/y was obtained. As shown in Figure 4, under the tubercle, selective corrosion, resulting in partial removal of iron, leaving spheroidal graphite is observed. Ductile iron coupon corrosion is a form of graphitic corrosion. This means that graphitic corrosion could be reproduced in the laboratory. Enrichment of Si and S in the corrosion residue in the pit can also be observed.

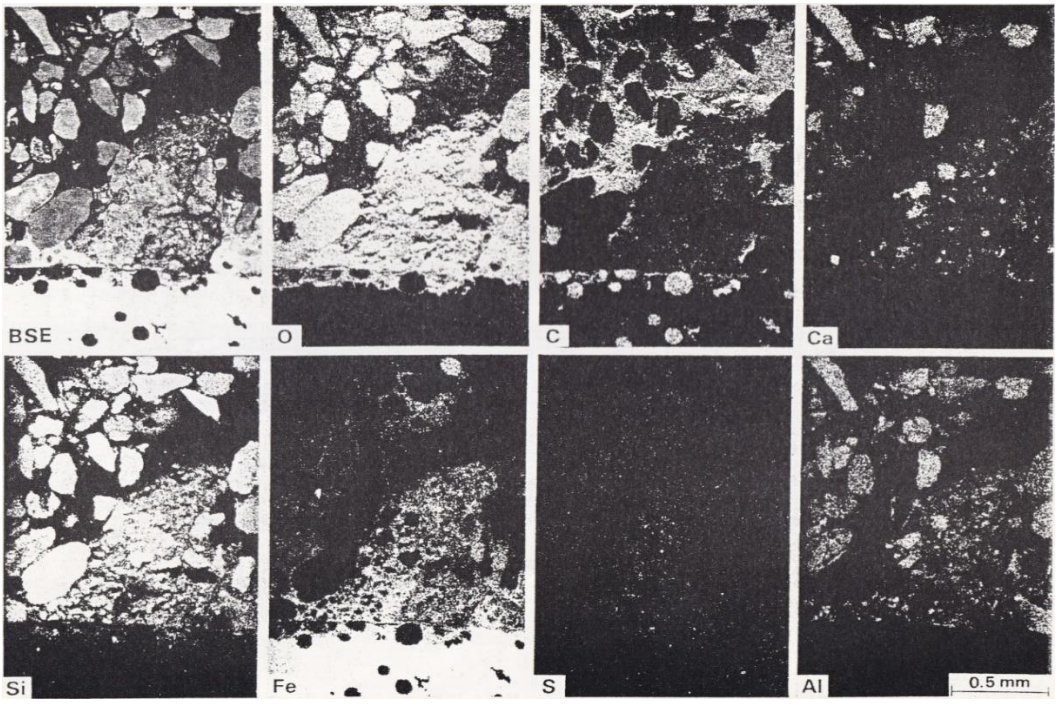


Figure 4 EPMA of a cross section of ductile iron coupon exposed for a period of 30 days to the soil shown in Table 2 [8].

### 4.6 General corrosion rate of ductile iron coupon from EIS data

EIS data may be used to determine charge transfer resistance $R_{ct}$, the inverse of corrosion rate. It is intelligible to express general corrosion rate as millimetre per year (mm/y) to provide an indication of penetration.

Kajiyama et al. applied electrochemical impedance spectroscopy (EIS) technique to monitor corrosion of ductile iron coupon in soil containing bacteria such as sulphate-reducing bacteria (SRB) , iron-oxidizing bacteria (IOB) and concluded that general corrosion rate could be estimated by the charge transfer resistance averaged over a period of 90 days as shown in Equation (1) using Faraday's Law :.

$$d = 130 / (R_{ct})_{av} \quad (1)$$

where

d : general corrosion rate (mm/y)

$(R_{ct})_{av}$ : the charge transfer resistance averaged over an extended periods ($\Omega cm^2$)

Figure 5 shows a fairly satisfactory relationship between general corrosion rate, d (mm/y) obtained from EIS data and that from mass loss measurement [10].

Therefore, $R_{ct}^{-1}$ is considered to be instantaneous general corrosion rate. In the case of ductile iron, the plots are a little bit deviated from the one-to-one line. This observation is interpreted as localized corrosion of ductile iron. From the measurement

on maximum depth of the ductile iron coupon, maximum corrosion rate was 0,487 mm/y.

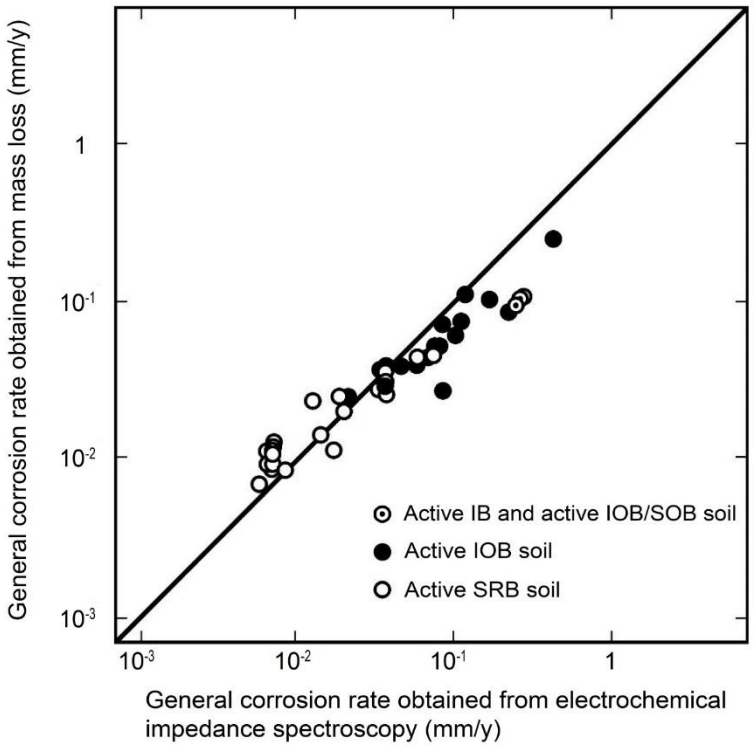


Figure 5 Relationship between general corrosion rate obtained from EIS data and that determined from mass loss measurements [11].
IB: iron bacteria
IOB: iron-oxidizing bacteria
SOB: sulphur-oxidizing bacteria
SRB: sulphate-reducing bacteria

### 4.7 Change in soil properties and $R_{ct}^{-1}$-time and $E_{corr}$-time data

Table 3 shows Change in burial environment observed in the laboratory burial testing. After testing, ion-oxidizing bacteria numbers at the interface between a working electrode and soil were found at levels a thousand-fold higher than bulk soil levels in association with sulphur-oxidizing bacteria and sulphate-reducing bacteria. At the same time, pH at the interface between a working electrode and soil after testing was found at levels a three-fold lower than bulk soil levels before testing. This observation supports situations which involve low pH usually indicate the activity of acid producing bacteria such as the *Thibacillus ferrooxidans* and/or *thiooxidans*. Low pH ensures that the surface within the pit remains active because the tubercle is permeable to the ions.

Table 3 Change in burial environment observed in the laboratory burial testing [9].

| Time (day) | Location | Eh ($mV_{SHE}$) | pH | Chemical species (mass ppm) | | | | | |
|---|---|---|---|---|---|---|---|---|---|
| | | | | $Fe^{2+}$ | FeS | $HCO_3^-$ | $SO_4^{2-}$ | $Cl^-$ | $NO_3^-$ |
| 0 | Bulk | 399 | 8,25 | 19 | 75 | 326 | 116 | 18 | 1 |
| 90 | Bulk | 374 | 7,23 | 83 | 20 | 200 | | | |
| | Electrode/soil | 399 | 5,61 | 147 | 27 | 271 | | | |

| Time (day) | Location | Bacteria (cell/g) | | | |
|---|---|---|---|---|---|
| | | IOB | SOB | IB | SRB |
| 0 | Bulk | 2×10 | Trace | ++ | 8×10 |
| 90 | Bulk | 8×10 | 2×10 | ++ | 4×10 |
| | Electrode/soil | $3×10^4$ | 9×10 | +++ | 3×10 |

+++ : very large, ++ : large

The $R_{ct}^{-1}$-time and $E_{corr}$-time data given in Figure 6 shows that high initial value and subsequent increased $R_{ct}^{-1}$ at an early stage suggested immediate initiation of corrosion occurred within 8 days of exposure to the soil. This indicates that soil was quite corrosive. From the results of EPMA, $R_{ct}^{-1}$-time, and soil properties, localized corrosion, that is graphitic corrosion, continues more readily in a ductile iron that is metallurgically heterogeneous in addition to the establishment of oxygen concentration cell in the initial stages. $E_{corr}$ is shifted in the positive direction corresponds to the process of graphitic corrosion.

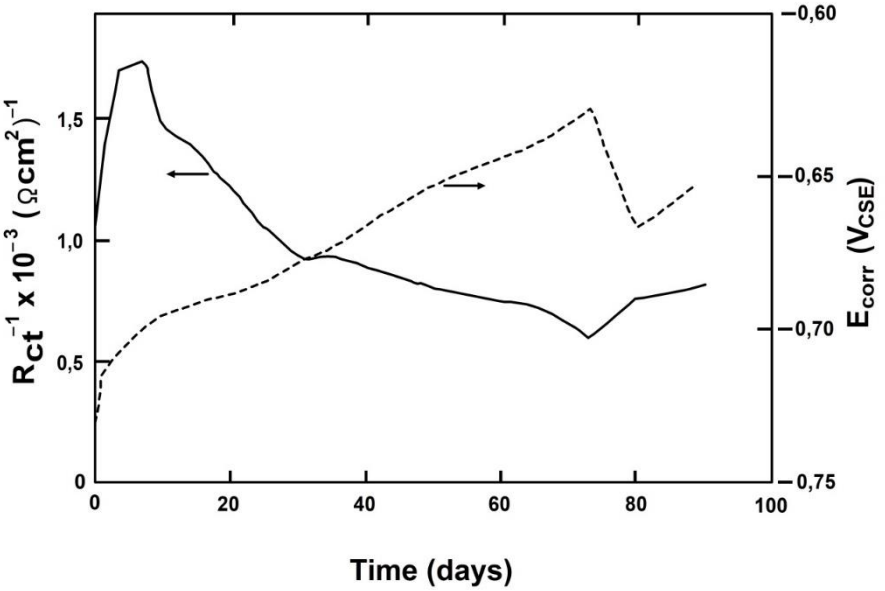


Figure 6 Typical results of the inverse of charge transfer resistance $R_{ct}^{-1}$ and corrosion potential $E_{corr}$ monitoring [9].

Change in EIS data with time is presented in Figure 7. The numbers on the impedance curve indicate the level of frequency at which the reading was taken. EIS data were basically capacitive in nature. As seen in Figure 6, after 30 days exposure notable decrease in $Rct^{-}$ was not observed. As shown in Figure 7, soil resistivity of 90 days exposure decreased compared with that of 30 days. The above-mentioned observations support that, in the corrosion pit, chemical and bacterial reactions acidified the environment, leading to continuous corrosion.

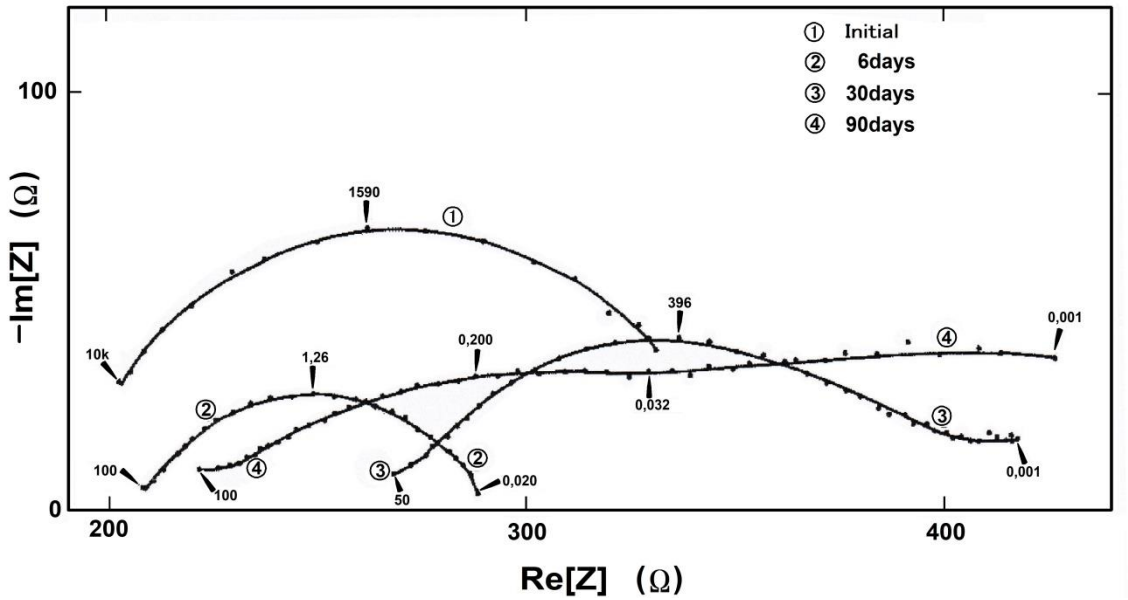


Figure 7 Change in EIS data with time in the laboratory burial testing on ductile iron coupon [9].

### 4.8 Polarization curves

Figure 8 shows polarization curves for ductile iron coupon at 25℃ in the soil shown in Table 3. Similar polarization curve after 90-day exposure is observed compared with the initial one. The extent of anodic polarization was taken to be nearly unchanged. Cathodic polarization curves represent sufficient cathodic reaction of oxygen, in accord with

$1/2O_2 + H_2O + 2e^- \rightarrow 2OH^-$.

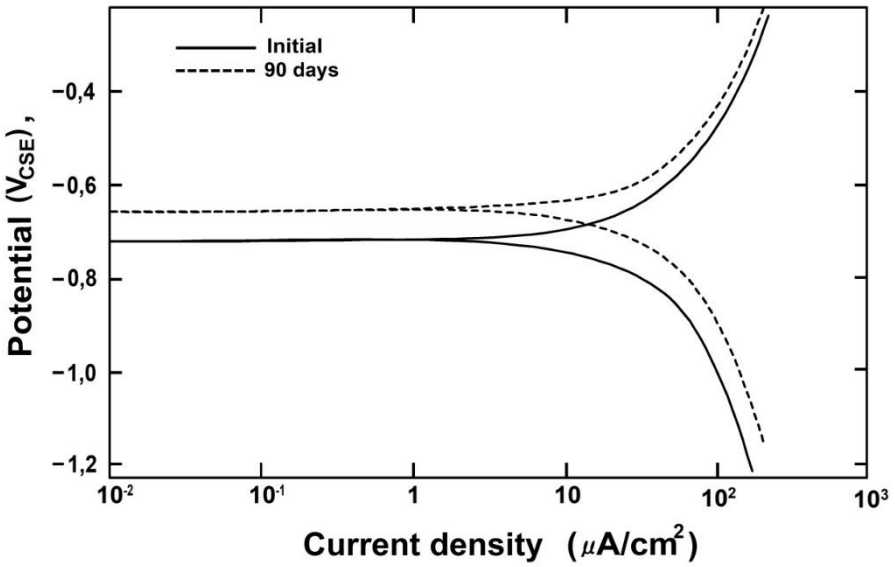


Figure 8 Potentiostatic polarization curves (Evans diagrams) for ductile iron coupon [9].

### 4.9 Mechanism on tubercle formation relevant to graphitic corrosion

Though graphitic corrosion of ductile iron pipe in fully anaerobic soil containing active SRB occurs, tubercle is not observed [1]. A question arises whether tubercle can be formed as long as soil is aerobic.

From the results from electrochemical measurements, electron probe microanalysis, X-ray diffraction, and bacterial culture, the mechanism on tubercle formation relevant to graphitic corrosion appears to be :

<Immediate initial corrosion subsequently the development of tubercle together with the growth of pit>

(1) localized corrosion continues more readily in ductile iron that is metallurgically heterogeneous in addition to the establishment of oxygen concentration cells ;

(2) At anodic site the following reaction proceeds.

$Fe \rightarrow Fe^{2+} + 2e^-$ ; (2)

(3) Cathodic reaction takes place at cathodic site.

$1/2O_2 + H_2O + 2e^- \rightarrow 2OH$ ; (3)

(4) A hydrolysis reaction of $Fe^{2+}$ occurs to form $Fe(OH)_2$ and $H^+$.

$Fe^{2+} + 2H_2O \rightarrow Fe(OH)_2 + 2H^+$ ; (4)

(5) $H^+$ ions react with $SO_4^{2-}$ ions which migrate towards the anode.

$2H^+ + SO_4^{2-} \rightarrow H_2SO_4$ ; (5)

(6) Partial $Fe^{2+}$ ions react with $SO_4^{2-}$ ions to provide $FeSO_4$ which are the substrate of IOB.

$Fe^{2+} + SO_4^{2-} \rightarrow FeSO_4$ ; (6)

(7) IOB grow utilizing $FeSO_4$ in the presence of $H_2SO_4$. Acidification by hydrolysis reaction and oxygen diffusion to the metal surface favour the activity of IOB.

$$FeSO_4 + 1/2H_2SO_4 + 1/4O_2 \xrightarrow{IOB} 1/2Fe_2(SO_4)_3 + 1/2H_2O \ ; \quad (7)$$

(8) A hydrolysis reaction of $Fe_2(SO_4)_3$ occurs to form $Fe(OH)_3$ and $H_2SO_4$ $Fe(OH)_3$ contributes to the formation of tubercle.

$Fe_2(SO_4)_3 + 6H_2O \rightarrow 2Fe(OH)_3 + 3H_2SO_4$ ; (8)

(9) A chemical attack of partial $Fe_2(SO_4)_3$ on Fe occurs generate the substrate of IOB, then the Equation (5) occurs.

$Fe_2(SO_4)_3 + Fe \rightarrow 3FeSO_4$ ; (9)

(10) The rest of $Fe^{2+}$ ions produced by anodic reaction react with $HCO_3^-$ ions (in soil solution) to form $FeCO_3$.

$Fe^{2+} + HCO_3^- \rightarrow FeCO_3 + H^+$ ; (10)

The insoluble $FeCO_3$ is trapped in the pit.

(11) $HCO_3^-$ ions play an important role in dissolving insoluble $FeCO_3$ in the pit, thereby generating $Fe(CO_3)_2^{2-}$ ions, the substrate of iron bacteria. Baylis reported that ferrous carbonate and calcium carbonate are insoluble compounds but that their solubility increases in the presence of bicarbonate ions [12].

$$FeCO_3 + HCO_3^- \rightarrow Fe(CO_3)_2^{2-} + H^+ ; \quad (11)$$

(12) IB utilise $Fe(CO_3)_2^{2-}$ to form FeOOH and $HCO_3^-$ ions

$$Fe(CO_3)_2^{2-} + 1/4O_2 + 3/2H_2O \xrightarrow{IB} FeOOH + 2\,HCO_3^- ; \quad (12)$$

Thus, the corrosion system is auto-catalytic with respect to $HCO_3^-$ ions, and thereby favouring rapid formation of tubercle accompanying appreciable graphitic corrosion.

Spontaneous oxidation reaction of $Fe^{2+}$ to $Fe^{3+}$ occurs gradually in the neutral to alkaline range. In the presence of active IB, the above oxidation reaction proceeds at much higher rate compared with the absence of IB.

Particularly in the corrosion pits, chemical and bacterial reactions acidify the environment leading to continuous corrosion. Accessibility of oxygen and permeability of ions to the ductile iron surface can favour the activities of IOB and IB, because densely packed and hard tubercles have not formed yet in the initial corrosion stages. <Stabilization of tubercle and pit relevant to graphitic corrosion>

(13) A very important, but little understood, process is the specific adsorption of $H_3SiO_4^-$ onto a positive charged goethite. $H_3SiO_4^-$ would be produced as follows :

Silica is one of the components of soil. Silicic acid which dissolves in alkaline soil water is produced by combining silica with soil solution ($SiO_2 + 2H_2O \rightleftarrows H_4SiO_4$) . Silicic acid is present mainly as orthosilicic acid, $H_4SiO_4$. The dissociation equilibrium reaction of $H_4SiO_4$ is :

$$H_4SiO_4 \rightleftarrows H^+ + H_3SiO_4^- \quad (13)$$

FeOOH is positively charged below pH 8-8,5 of the zero point of charge (ZPC) [13]. It is probable that the stabilized formation of tubercle and pit is the result of specific adsorption of negatively charged $H_3SiO_4^-$ onto a positively charged FeOOH, the coexisting opposite charges tending to stabilize the tubercle and pit according to Equation (14) .

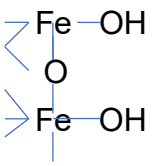


$+ H_3SiO_4^- \rightarrow$ coordinate bond [increase of negative charge] (14)

The above-mentioned consideration supports the EPMA observations, that is, the distribution of Fe coincided with that of Si together with O, thereby sustaining the insoluble and stable tubercle and pit.

## 5 Conclusions

1) Ductile iron corrosion is a form of graphitic corrosion.
2) Bicarbonate ions ($HCO3^-$) provide $Fe(CO_3)_2^{2-}$ ions as substrate of iron bacteria (IB), resulting in the formation of goethite (FeOOH).
3) Pits develop as a form of graphitic corrosion within the growing tubercles which are permeable to some ions involved in the corrosion process.
4) It is probable that the stabilized formation of tubercle and pit is the result of specific adsorption of negatively charged $H_3SiO_4^-$ onto a positively charged FeOOH, the coexisting opposite charges tending to stabilize the tubercle.

## References


[1] F. Kajiyama, “Extensive investigation into ductile-iron natural gas pipeline corrosion in soils,” CEOCOR 2019, Denmark, Copenhagen, paper 2019-19, 1−16 (2019).

[2] NACE International, “Corrosion and Corrosion Control for Buried Cast- and Ductile-Iron Pipe,” p.11 (2013).

[3] Ductile Iron Pipe Research Association, “Corrosion Control Polyethylene Encasement,” p.7 (2017).

[4] American Water Works Association, AWWA, “AWWA C 105-10 Polyethylene encasement for ductile-iron pipe systems, ” (2010).

[5] DIN 50 929, “Korrosionswahrscheinlichkeit metallischer werkstoffe bei äußerer Korrosionsbelastung Rohrleitungen und Bauteile in Böden und Wässern,” (1985).

[6] J. R. Postgate, “The Sulphate-reducing Bacteria,” Cambridge University Press (1979).

[7] F. Kajiyama, “A doctoral thesis,” Tokyo Institute of Technology (1989).

[8] K. Kasahara, F. Kajiyama, “The Role of Bacteria in the Graphitic Corrosion of Buried Ductile Cast Iron Pipes, ”Microbial Corrosion, Proceedings of the 2nd EFC Workshop, Edited by C. A. C. Sequeira and A. K. Tiller, Portugal, p.235 (1992).

[9] K. Kasahara, F. Kajiyama, K. Okamura, “The Role of Bacteria in the Graphitic Corrosion of Buried Ductile Cast Iron Pipes, ” *Zairyo-to-Kankyo*, 40, p.806 (1991).(in Japanese)

[10] M. Igarashi, K. Sato, “The world’s first elucidation of orthosilicic axid, basic unit of glass, ” Research results, Interdisciplinary Research Center for Catalytic

Chemistry, National Institute of Advanced Industrial Science and Technology (2017)
[11] F. Kajiyama, K. Okamura, Y. Koyama, K. Kasahara, “Microbiologically influenced corrosion (MIC) of ductile iron pipes in soils,” Microbiologically influenced corrosion testing, J. R. Kearns/B. J. Little editors, ASTM, p.266 (1994).
[12] J. R. Baylis, “Factors other than dissolved oxygen influencing the corrosion of iron pipes, “ Ind. Eng. Chem. 18, 370 (1926).
[13] “Acid soil and its agricultural utilization,” Hakuyusha, Akira Tanaka ed. (1984). (in Japanese)